Molecular Biology of the Cell
Vol. 21, 2788–2796, August 1, 2010

Glycogen Synthase Kinase-3 Is Required for Efficient *Dictyostelium* Chemotaxis

Regina Teo,* Kimberley J. Lewis,† Josephine E. Forde,‡ W. Jonathan Ryves,* Jonathan V. Reddy,* Benjamin J. Rogers,* and Adrian J. Harwood*

*Cardiff School of Biosciences, Cardiff University, CF10 3AX Cardiff, United Kingdom; †Cardiff School of Medicine, Cardiff University, CF14 4XW Cardiff, United Kingdom; and ‡Swansea University, SA2 8PP Swansea, United Kingdom

Submitted October 26, 2009; Revised May 25, 2010; Accepted June 1, 2010
Monitoring Editor: Carole Parent

Glycogen synthase kinase-3 (GSK3) is a highly conserved protein kinase that is involved in several important cell signaling pathways and is associated with a range of medical conditions. Previous studies indicated a major role of the *Dictyostelium* homologue of GSK3 (*gskA*) in cell fate determination during morphogenesis of the fruiting body; however, transcriptomic and proteomic studies have suggested that GSK3 regulates gene expression much earlier during *Dictyostelium* development. To investigate a potential earlier role of GskA, we examined the effects of loss of *gskA* on cell aggregation. We find that cells lacking *gskA* exhibit poor chemotaxis toward cAMP and folate. Mutants fail to activate two important regulatory signaling pathways, mediated by phosphatidylinositol 3,4,5-trisphosphate (PIP_3) and target of rapamycin complex 2 (TORC2), which in combination are required for chemotaxis and cAMP signaling. These results indicate that GskA is required during early stages of *Dictyostelium* development, in which it is necessary for both chemotaxis and cell signaling.

INTRODUCTION

Glycogen synthase kinase-3 (GSK3) is a multifunctional protein kinase that is highly conserved throughout the eukaryotes. In animals, including humans, it is associated with important embryological and physiological signaling processes, such as Wnt and insulin signaling (Cross *et al*., 1995; Papkoff and Aikawa, 1998). As a consequence it is linked to major clinical conditions, including cancer, diabetes, and Alzheimer's disease. At the cellular level GSK3 mediates processes, such as regulation of gene expression, control of proteolysis, metabolism, and control of the cytoskeleton (Harwood, 2001; Kim *et al*., 2002). The question of how GSK3 exerts its effects on these multiple processes is important for understanding the integration of cell signaling within the cellular context.

The social amoeba *Dictyostelium* grows and divides in the presence of nutrients in a unicellular form, but when starved it undergoes a developmental program to form a multicellular and differentiated structure, termed the fruiting body (Harwood, 2001). *Dictyostelium* development comprises of two major phases. First, during aggregation phase, cells migrate together by chemotaxis in a process mediated by cAMP pulses. Second, the multicellular aggregate, or mound, undertakes a series of differentiation events and morphogenetic movements to ultimately form a fruiting body, which comprises spore cells within a spherical head, supported by a stalk of vacuolated, cellulose encased stalk cells.

Dictyostelium possesses a single homologue of GSK3, *gskA* (Harwood *et al*., 1995). It was discovered previously that GskA regulates the processes that control cell fate (Harwood *et al*., 1995). This initially occurs during early stages of multicellular development, when cells first come together to form a multicellular mound. At this point, cells differentiate into three basic cell types; prespore cells that eventually form spores, and prestalk cells (pst) comprising pstA cells that give rise to the stalk and the majority of its associated structures and pstB cells that form the basal disk that anchors the stalk to the substratum (Williams *et al*., 1989). In wild-type cells, 80% of the cells form prespore cells and the remainder form pst cells, of which the majority are pstA. However, in a *gskA* null mutant, the pstB population expands at the expense of the prespore population, so that the final fruiting body of the basal disk is greatly enlarged and the spore head reduced (Harwood *et al*., 1995). During later stages of fruiting body formation, GskA regulates a second cell fate decision by controlling the differentiation from pstA cells to pstAB cells (Schilde *et al*., 2004), which progress to form the main structural element of the stalk.

In the mound, activation of GskA is mediated by high concentrations of cAMP via the cAMP receptors carC and carD, which control tyrosine phosphorylation of GskA by the kinase ZakA (Kim *et al*., 1999) and an unidentified tyrosine phosphatase (Kim *et al*., 2002). Downstream of GskA lies a β-catenin homologue, Aardvark (Aar; Grimson *et al*., 2000), and a signal transducer and activator of transcription (STAT) transcription factor, STATa (Ginger *et al*., 2000), although the full role of these proteins is currently unclear.

Although the phenotypes described for *gskA* null mutants occur during multicellular stages, GskA expression and ac-

This article was published online ahead of print in *MBoC in Press* (http://www.molbiolcell.org/cgi/doi/10.1091/mbc.E09–10–0891) on June 9, 2010.

Address correspondence to: Regina Teo (teor@cardiff.ac.uk).

Abbreviations used: GSK3, glycogen synthase kinase-3; PIP_3, phosphatidylinositol 3,4,5-trisphosphate; TOR, target of rapamycin; TORC2, target of rapamycin complex 2.

tivity is present throughout *Dictyostelium* development (Plyte *et al*., 1999). A proteomic and microarray analysis of cells at 5 h of development, several hours before the first multicellular developmental stages, revealed ≈150 genes with altered patterns of expression (Strmecki *et al*., 2007). Curiously, of those genes identified that had been characterized previously, all are associated with growth and aggregation phase rather than multicellular development. This raises the question of additional roles of GskA during these earlier stages of *Dictyostelium* development.

Here, we report an in-depth investigation of aggregation and chemotaxis of *gskA* null mutants. We find that *gskA* null mutant cells have defective chemotaxis toward cAMP and folate, a growth phase chemoattractant. The chemotaxis defect is accompanied by suppression of phosphatidylinositol 3,4,5-trisphosphate (PIP_3) levels. However, we observe that loss of *gskA* causes a much greater effect on cAMP-mediated chemotaxis than can be accounted for by loss of PIP_3 signaling alone (Lee *et al*., 2005; Hoeller and Kay, 2007; Takeda *et al*., 2007). We find that protein kinase B (PKB)R1 is not phosphorylated in *gskA* mutants, a protein kinase related to PKB but regulated in a PIP_3-independent manner. Loss of both PIP_3 signaling and PKBR1 phosphorylation has a strong effect on chemotaxis. Finally, we show that *gskA* null mutant cells do not generate cAMP pulses during aggregation, demonstrating that GskA plays a major role in the regulation of chemotaxis and early *Dictyostelium* development.

MATERIALS AND METHODS

Strains

The *gskA* null strain (ID Strain: DBS0236114) was obtained from the Dicty Stock Centre (http://dictybase.org/) and was originally generated in the *Dictyostelium discoideum* strain AX2 background. The wild-type strain refers to AX2 and is the same strain denoted in Bloomfield *et al*. (2008). Cells were cultured axenically on plates in HL5 with glucose medium (Formedium HLG0102) before experiment. *gskA* null mutants were grown in media supplemented with 10 μg/ml blasticidin, and *gskA* null transformants carrying GskA-green fluorescent protein (GFP) (*gskA*-GSKA) and immobilized metal assay of phosphorylation (IMPA)-GFP (*gskA*-IMPA) were grown in medium supplemented with 40 μg/ml G418 (catalog no. 11811–023; Invitrogen). All cells were maintained at 22°C.

Plasmids

The GskA-GFP2 rescue protein for *gskA* was constructed by inserting the coding regions of GskA into pDXA GFP2 at the Kpn1 and Nsi1 restriction sites, such that the fusion protein was expressed under the control of a constitutive Actin15 promoter. By introducing point mutations into the coding region of the pDXA GskA-GFP2, the kinase-dead construct pDXA GskA-GFP2 K85R was made with the QuikChange site-directed mutagenesis kit (Strategene , La Jolla, CA) as per the manufacturer's direction. The coding sequence of the *IMPA* gene was amplified from the cDNA clone FCBP15, obtained form the Japanese *D. discoideum* cDNA project (Morio *et al*., 1998). The insert was subsequently ligated into the pTX-GFP vector.

Cell Signaling Assays

cAMP was measured as described previously (Snaar-Jagalska and Van Haastert, 1994) by using isotope dilution assay kits (GE Healthcare, Little Chalfont, Buckinghamnshire, United Kingdom). Cells were starved in KK2 buffer (6.5 mM KH2PO4, 3.8 mM K2HPO4, pH 6.2) for 5 h in shaking culture at a concentration of 1×10^7 cells/ml. To determine cAMP levels, cells were resuspended at 5×10^7 cells/ml, and 100 μl of cells was stimulated with 5 μM 2′-deoxy-cAMP in the presence of 5 mM dithiothreitol. Reactions were terminated by the addition of 100 μl of 3.5% (vol/vol) perchloric acid on ice. Samples were neutralized with 50 μl of $KHCO_3$ (50% saturated), followed by centrifugation for 2 min at 14,000 × *g* at 4°C. Finally, 50 μl of each sample was added to the cyclic AMP ^{3}H assay system (GE Healthcare).

Wild-type cells transformed with the plasmid WF38 (PHCRAC-GFP; Parent *et al*., 1998) were pulsed with cAMP for 5 h with an end concentration of 100 nM. Cells were subsequently stimulated by the addition of 1 μM cAMP, and protein translocation was recorded by fluorescence videomicroscope with a 60× objective.

Time-Lapse Analysis

For chemotaxis to folate, cells were grown axenically to a density of 1×10^6, and 4×10^5/cm^2 cells were washed twice in 20% media/KK2 and replated in a LabTek coverglass chambered well (Nunc 155379; Nalge Nunc International, Rochester, NY) with 2 ml of 20% media/KK2. Folate (25 mM) was delivered via a Femtotip (5242 952.008; Eppendorf, Hamburg, Germany), and images were recorded for every 20 s under 10× phase objective. For aggregation, 5×10^6 cells were washed and plated on KK2 agar. Images were taken every 30 s for cAMP pulse movies under 4× objective for at least 24 h. Postprocessing was carried out with ImageJ (National Institutes of Health, Bethesda, MD). For chemotaxis, 5×10^7 cells were shaken in KK2 buffer (Formedium KK29907) for 5 h while being pulsed every 6 min with cAMP to an end concentration of 10^{-7} M. The chemotaxis-competent cells were placed in a Zigmond chamber (Z02; Neuro Probe, Gaithersburg, MD) in a cAMP gradient (source at 10^{-6} M cAMP, sink with no cAMP). Differential interference contrast images of cells were captured with a 20× objective at 6-s intervals for 15 min. Cell movement was analyzed using Dynamic Image Analysis System (DIAS), version 3.4.1 (Soll Technologies, Iowa City, IA; Curreli *et al*., 2001). Statistical analysis was carried out using the nonparametric Kruskal–Wallis test, with a post hoc Dunn's multiple comparison test using Prism 4 (GraphPad Software, San Diego, CA).

Phospholipid Radiolabeling and Thin Layer Chromatography (TLC) Analysis

Cells (1×10^8) were starved and pulsed for 4 h with 100 nM cAMP. At the fourth hour, cells were pelleted and resuspended in 600 μl of KK2. Radioactive [γ-^{32}P]ATP was added (1.2 MBq), and the cells were pulsed with cAMP for a further hour (100 nM/6 min).

Phospholipids were extracted as described in Konig *et al*. (2008): cells were added to 750 μl of acidified A (chloroform/methanol/HCl (1M) ratio: 40:80:1) and sonicated. A further 250 μl of chloroform and 450 μl of 1 M HCl were added to the cells, and then the cells were vortexed and spun, and the lower phase was collected. The process was repeated two more times, once with chloroform/methanol/HCl (1M) (ratio: 10:10:4) and the second time with methanol/EDTA (100 mM) (ratio: 1:0.9) and subsequently dried. Samples were then resuspended in chloroform/methanol (ratio: 2:1) and spotted onto a TLC plate (Cole-Parmer Instrument, Vernon Hills, IL). Plates were developed with a chloroform/acetone/methanol/acetic acid/double-distilled H_2O solvent system (ratio 46:17:15:14:8), and phospholipids were visualized by spraying with molybdenum Blue spray reagent (Sigma Chemical, Poole, Dorset, United Kingdom). Radiolabeled lipid spots were imaged by exposing the plate to Hyperfilm (GE Healthcare) for 3 d. PIP_3 measurements were carried out according to manufacturer's instructions (K-2500s PIP_3 Mass ELISA kit; Echelon Biosciences, Salt Lake City, UT). Anti-phospho protein kinase C (PKC; pan) antibody used for detection of PKBA and PKBR1 was purchased from Cell Signaling Technology (190D10; Danvers, MA) and analyzed as described previously (King *et al*., 2009).

Quantitative Reverse Transcription-Polymerase Chain Reaction (qRT-PCR)

Dictyostelium cells were starved and shaken with pulses of 100 nM cAMP for 5 h. Cells (2×10^6) were then harvested and pellets were snap-frozen. RNA was isolated using an illustra RNA spin mini kit (25-0500-72; GE Healthcare), and its integrity was checked on a 1% formaldehyde agarose gel. Genomic DNA contamination was checked by PCR using existing primers for a known gene. cDNA was prepared using the First-Strand cDNA kit (11483188001; Roche Diagnostics, Mannheim, Germany) using 1 μg of RNA and random primers. A minus-reverse transcriptase control was also set up. qRT-PCR was carried out on a Chromo4 machine (Bio-Rad laboratories, Hercules, CA) with the Opticon2 detection software. The fluorophore used for detection was SYBR Green. iq SYBR Green master mix (170-8884; Bio-Rad Laboratories) was used for the reactions with 100 μg of cDNA. Housekeeping genes incorporated for quantification were *lg7* (www.dictybase.com; ID Strain: DDB_G0294034), *impk1*, and *impk2*. The genes of interest were *carA-1* (DDB_G0273397), *acaA* (DDB_G0281545), and *pdsA* (DDB_G0285995). Data analysis was carried out using the qbase software Jo VandeSomple and Jan Hellemans (Hellemans *et al*., 2007). Standard curves were created for all genes by using a 3-point 10-fold dilution series of Ax2 0 h cDNA, and all samples also were normalized to the Ax2 0 h cDNA. Primer sequences are as follows: *ig7 forward*, TCCAAGAGGAAGAGGAGAACTGC and *ig7 reverse*, TGGGGAGGTCGTTACACCATTC; *ipmk1 forward*, GCAGGTTCAACACCATTCAAAAAATC and *ipmk1 reverse*, TCCAACACTATCCATTCCTTACCATC; *ipmk2 forward*, TGGTAGTTTTTTGAGTGTCAGCCC and *ipmk2 reverse*, TGATGATGTTGTTGTTGTTG TTGTAGTG; *carA-1 forward*, ATGTTGGGTTGTATGGCAGTG and *carA-1 reverse*, AGGGAAACCACCATTGACAG; *acaA forward*, CATTCTAGAGGCGGTATTGGC and *acaA reverse*, GGAGAAAATGTCTGATTTCGCTT; and *pdsA forward*, CCATTGGGTACAACTGGTGGA and *pdsA reverse*, AACTGCCCATGATGGATAGGT.

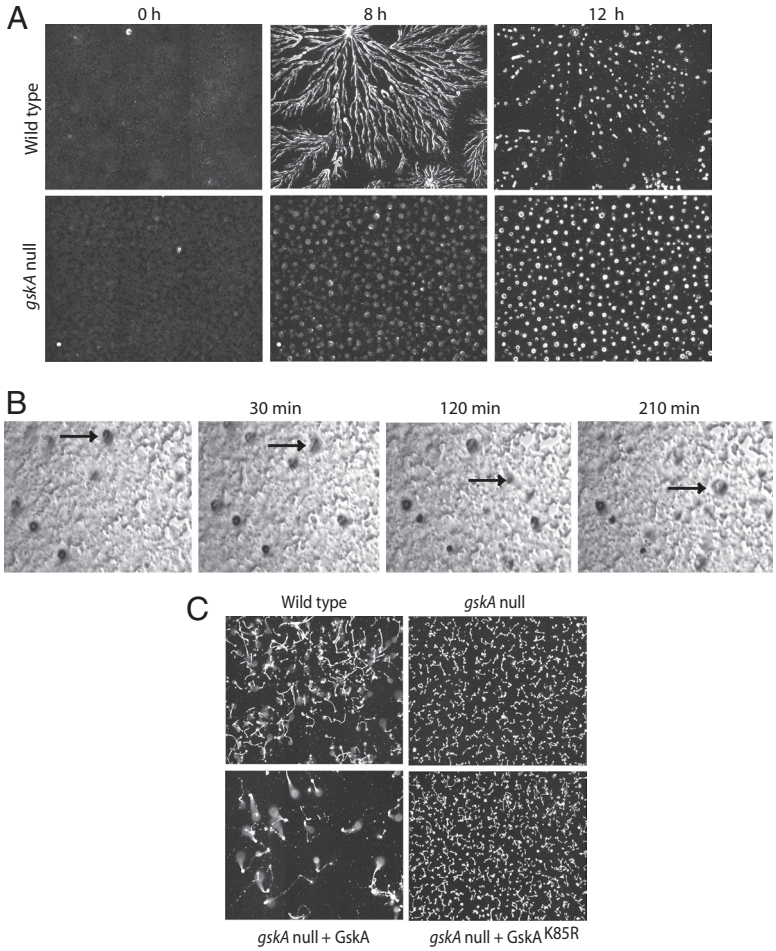

Figure 1. Analysis of *Dictyostelium* development. (A) Wild-type cells form streams ~8 h after starvation, but *gskA* null mutants bypass this stage and form small mounds that are unstable. (B) Mounds of *gskA* null mutant cells are constantly disaggregating and reaggregating. Arrows indicate mounds exhibiting this process. (C) *gskA* null mutant cells carrying a rescue plasmid proceed normally through development (bottom left), but a kinase-dead version ($GskA^{K85R}$) in the *gskA* null mutant had similar development to the original null, indicating a requirement for kinase activity for normal development.

RESULTS

gskA Null Mutants Have Aberrant Aggregation

We observed previously that *gskA* null mutant cells had unusual aggregation, forming small mounds ~2 h before wild-type strains. This was independent of parental background, being seen in mutants created from both DH1 and AX2 parental wild-type strains (Harwood *et al*., 1995; Schilde *et al*., 2004). Small mounds also were seen in cells treated with lithium, an inhibitor of GSK3 (Williams *et al*., 1999). This prompted a more in depth investigation of *gskA* null mutants.

To investigate the role of GskA during aggregation, wild-type and *gskA* null mutant cells were plated for development and recorded using time-lapse videomicroscopy. As seen previously, *gskA* null mutant cells formed small mounds ≈2 h earlier than wild-type cells (Supplemental Movie 1). These small mounds formed without the multicellular streams seen in wild-type cells (Figure 1A). Furthermore, the small mounds were unstable, and they often disaggregated before reaggregating in different positions on the substratum (Figure 1B). Restoring GskA activity via expression of the wild-type *gskA* cDNA in *gskA* null mutants, rescued aggregation to that seen in the wild type (Figure 1C). However, no phenotypic rescue was seen after expression of a mutant gene that lacks kinase activity ($GskA^{K85R}$), indicating a requirement for kinase activity to mediate GskA function (Figure 1C).

GSK3 Is Required for Chemotaxis to cAMP and Folate

We tested the ability of *gskA* null cells to undergo chemotaxis to cAMP. Cells were pulsed with cAMP for 5 h and then placed in a gradient formed from a 1 μM cAMP source. *gskA* null mutant cells had a complete loss of chemotaxis. Cell chemotaxis can be measured as the chemotactic index (CI), where +1 represents maximally accurate chemotaxis toward the cAMP source, −1 represents chemotaxis away from the cAMP source, and 0 is random movement neither toward nor away from the cAMP source. We also have calculated the percentage of cells that respond positively toward cAMP (% cells respond), and this represents the proportion of cells that have CI values of ≥0.7, with $\cos^{-1}(0.7) = 45°$ and $\cos^{-1}(1.0) = 0°$. Hence, cells with CI = 1.0, chemotax in a straight line to cAMP, whereas any cell that deviates 45° on either side of this would exhibit a value of 0.7.

Wild-type cells possessed a mean CI of 0.9, with 88.7% of wild-type cells exhibiting chemotaxis toward cAMP compared with 31.5% of *gskA* mutant cells. This is a slightly higher percentage (25%) than expected from cells when they randomly move. The *gskA* null mutant cells have a strongly decreased mean CI value of 0.18 and in addition exhibited an approximate 50% decrease in cell speed and directionality, a measure of cell turning as they migrate toward the cAMP source. Re-expression of GskA in the *gskA* null mutant restores CI, cell speed, and directionality to that of the

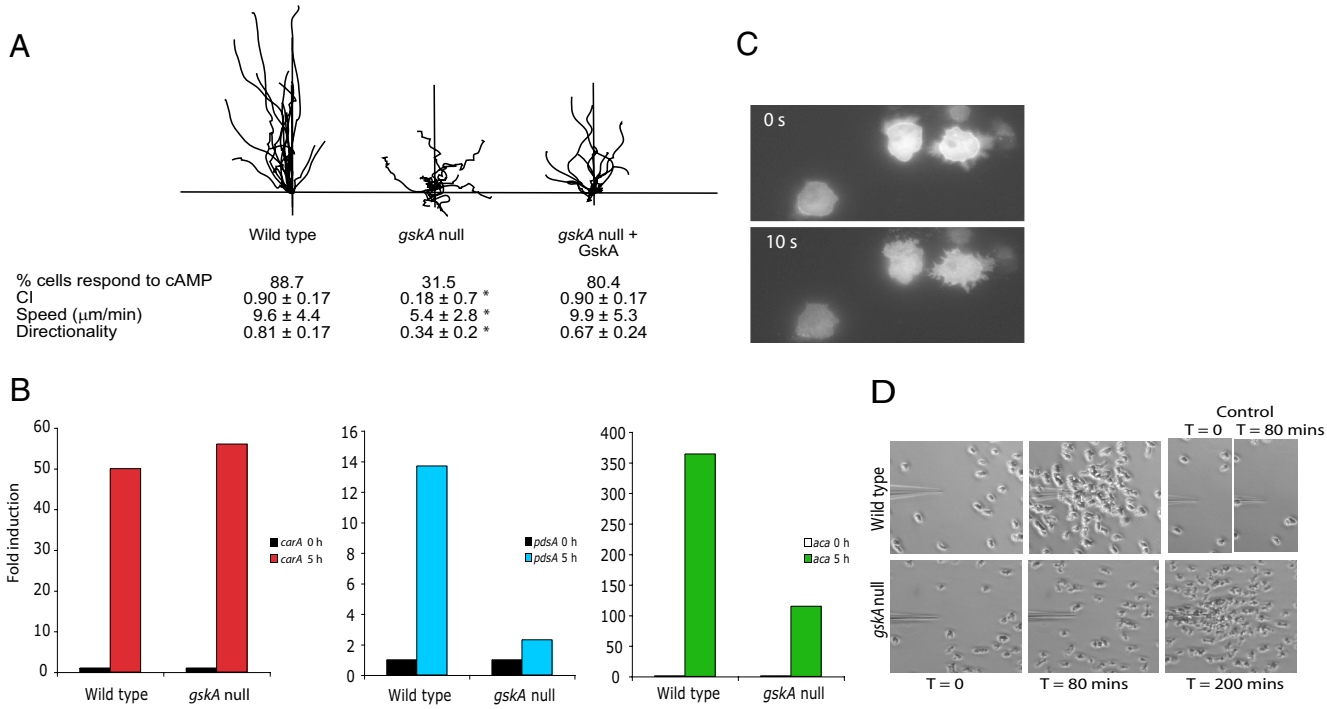

Figure 2. Chemotaxis of *gskA* null mutant cells. (A) Chemotaxis parameters for wild-type, *gskA* null mutant, and *gskA* null cells expressing GskA (*gskA*-GskA). "% cells respond to cAMP" indicates the proportion of cells that have a CI values of ≥0.7, with $\cos^{-1}(0.7) = 45°$ and $\cos^{-1}(1.0) = 0°$. Values are means and SDs based on at least 140 cells, compiled from three independent experiments. Dunn's multiple comparison's test between wild type and *gskA* null mutant showed a significant difference at $p < 0.001$ for all three parameters. (B) qRT-PCR showed gene induction for *carA*, *pdsA*, and *aca* are to similar levels to that observed in the earlier microarray study (Strmecki *et al*., 2007). The *y*-axes denote fold induction. (C) *gskA* null mutant cells are able to cause PTEN-GFP relocalization within 10 s of cAMP stimulation. (D) Chemotaxis to 25 mM folate. Wild-type cells take on average 140 min to show clustering at the micropipette compared with *gskA* null mutants, taking an average of 270 min. Figures here show a representative of one replicate experiment. Control, buffer used to dissolve folate.

wild-type cells. These results indicate a strong chemotaxis defect toward cAMP in the *gskA* null mutant (Figure 2A).

To exclude the possibility that the cells could not sense cAMP, we examined expression of genes involved in chemotaxis and cell signaling. The earlier microarray was carried out in cells that had been starved for 5 h and matched the developmental state of those used in our chemotaxis experiments (Strmecki *et al*., 2007). We reexamined the results of the microarray but failed to detect differences in gene expression of the cAMP receptor genes. *carA* is the major receptor expressed during aggregation (Sun and Devreotes, 1991), and we used qRT-PCR to confirm that there was no difference in *carA* gene expression between wild-type and *gskA* null mutant cells (Figure 2B). The microarray showed altered expression of *pdsA* and *pdiA* genes, all which play a role in aggregation and we confirmed that induction of *pdsA*, which encodes a cAMP phosphodiesterase, is indeed substantially reduced in *gskA* null cells (Figure 2B). Finally, a survey of major genes expressed during aggregation showed that the expression of the adenylyl cyclase *acaA* gene was induced to only 30% of the wild type. This may have been below the threshold to detect on the microarray (Figure 2B).

To confirm that *gskA* null cells can sense and respond to cAMP, we examined the response of phosphatase and tensin homologue (PTEN) to cAMP stimulation. In wild-type cells, an accumulation of PTEN protein was seen on the cell membrane but was lost to the cytosol within seconds of cAMP accumulation. This relocalization was still present in *gskA* null cells (Figure 2C), demonstrating that the loss of *gskA* did not block cAMP sensing and some downstream events.

To examine chemotaxis in a context independent of cAMP signaling, we investigated the ability of the *gskA* null mutant to chemotax toward folate. This occurs during growth of *Dictyostelium* where cells are attracted to folic acid and pterins (Pan *et al*., 1972, 1975), substances that are secreted by bacteria, the *Dictyostelium* food source. We recorded the chemotaxis response of growth phase cells to 25 mM folic acid, delivered via a micropipette. We again observed a substantial chemotaxis defect in *gskA* null cells compared with wild type (Figure 2D). Together, these results indicate a requirement of GskA in *Dictyostelium* chemotaxis.

GSK3 Is Required for PIP_3 Signaling

To investigate the chemotaxis deficit in *gskA* null mutant cells during early development, we examined PIP_3, a downstream effector of cAMP and mediator of the chemotaxis response. To do this, we monitored phosphorylation of PKBA, the *Dictyostelium* homologue of PKB. As in its animal homologues, PKBA contains a pleckstrin homo0logy (PH)-domain that mediates translocation to the plasma membrane via PIP_3 binding, where the protein is subsequently phosphorylated (Kamimura *et al*., 2008). It therefore is a good monitor for PIP_3 synthesis after cAMP stimulation. In wild-type cells, PKBA phosphorylation occurred within seconds of cAMP stimulation, with a peak between 10 and 20 s, and then declined to basal levels by 60 s. No cAMP stimulated elevation of PKBA occurred in *gskA* null mutant cells (Figure 3A). We can exclude a failure to express the *PKBA* gene because no difference in expression between mutant and

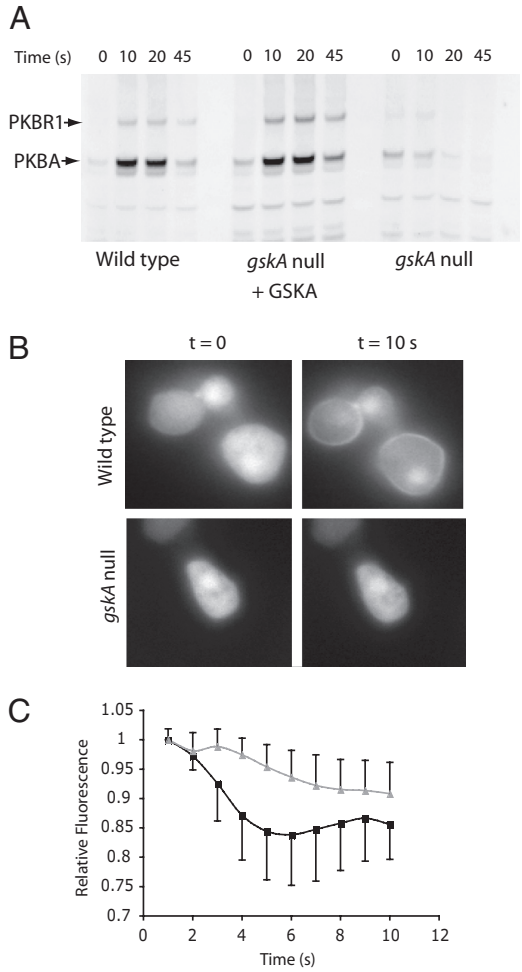

Figure 3. PKB phosphorylation is lost in *gskA* null mutant cells. (A) Phosphorylation of PKBA on T278, indicative of PIP_3 synthesis (bottom arrow) peaks at 10 s post cAMP stimulation in the wild type and *gskA*-GskA but not the *gskA* null mutant. Phosphorylation of PKBR1 on T309 (top arrow) showed kinetics similar to that for T278 for both wild type and *gskA*-GskA and again is not observed for the *gskA* null mutant. (B) PH_{crac}-GFP translocation to the membrane is not observed in the *gskA* null mutant; however, relative fluorescence profiles post-cAMP stimulation showed small cytosolic fluorescence loss but not to the extent that observed for the wild type (C).

wild-type cells was observed either in the microarray (Strmecki *et al*., 2007) or by qRT-PCR (data not shown).

To pursue this further, we monitored PIP_3 synthesis in living cells by expression of the PIP_3-specific binding protein PH_{CRAC}-GFP (Parent *et al*., 1998). When cells are stimulated with a global cAMP signal, PIP_3 is generated on the entire plasma membrane, causing translocation of PH_{CRAC}-GFP from the cytosol to the membrane. In wild-type cells, PH_{CRAC}-GFP was recruited to the membrane within 10 s of cAMP addition and is subsequently lost after 30 s. No PH_{CRAC}-GFP membrane translocation was observed in the *gskA* null cells (Figure 3B) and when levels of fluorescence were quantified, PH_{CRAC}-GFP was suppressed to only 10% of that seen in wild-type cells (Figure 3C).

Increasing PIP_3 Levels Rescues Chemotaxis in the gskA Null Mutant

We previously showed that overexpression of the inositol monophosphatase gene IMPA in wild-type cell elevates PIP_3 by increased synthesis of the phosphatidylinositol 3-kinase (PI3-kinase) substrate phosphatidylinositol 4,5-bisphosphate (PIP_2; King *et al*., 2009). We used IMPA overexpression to elevate PIP_3 in *gskA* null cells and examined its effects. Overexpression of IMPA in *gskA* null mutant cells not only rescued chemotaxis, restoring mean cell speed, directionality, and CI values of *gskA* null mutant cells to wild-type control values (Figure 4A), it also restored PKBA phosphorylation (Figure 4B). This not only indicated that GskA plays a major role in PIP_3 signaling, it again demonstrated that *gskA* null mutant cells could sense sufficient cAMP to restore chemotaxis when this downstream effector is restored.

We used IMPA overexpression to probe how loss of *gskA* affects PIP_3 signaling. One possibility is that GskA regulates IMPA activity or other targets on the inositol–PIP_2 pathway. A lack of PIP_2 would then lead to a decrease in PIP_3 synthesis, in a similar mechanism to that seen with lithium treatment (King *et al*., 2009). In contrast, elevation of PIP_3 may bypass a block in an alternative pathway, such as activation of PI3-kinase. We measured synthesis of phosphatidyl inositol phosphates (PIPs) in wild-type, *gskA* null mutant, and *gskA* null mutant IMPA-overexpressing cells. We observed no difference in phosphatidylinositol (PI), phosphatidylinositol phosphate (PIP), and PIP_2 synthesis between wild-type and *gskA* null mutant cells (Figure 4C). This argued against a requirement for GskA for PIP_2 synthesis. In contrast, we saw an increase in PIP_2 in *gskA* null mutant IMPA-overexpressing cells (Figure 4C). This suggested that IMPA overexpression bypasses a deficit in PIP_3 signaling by elevating PIP_2 and hence PIP_3 synthesis.

Finally, we measured PIP_3 directly and found that in response to cAMP, *gskA* null mutant cells did not synthesize PIP_3 but seemed to lose it. This response is the opposite to that observed in either wild-type or *gskA* null mutant IMPA-overexpressing cells (Figure 4D), which rapidly synthesize new PIP_3 under these conditions. Overall, the data showed that very little PIP_3 is formed in *gskA* null mutant cells.

GskA Is Required for Target of Rapamycin Complex 2 (TORC2)-mediated Signaling

We noted that the cAMP chemotaxis phenotype seen in the *gskA* null mutant was much stronger than that observed for loss of PIP_3 signaling alone (Hoeller and Kay, 2007; Takeda *et al*., 2007; King *et al*., 2009), and sought evidence for a further molecular defect in the *gskA* null mutant. Previously, it has been found that signaling via the kinase target of rapamycin (TOR) acting in the TORC2 complex was capable of mediating cAMP chemotaxis when PIP_3 synthesis was inhibited (Kamimura *et al*., 2008). This alternative chemotaxis mechanism acts via a second PKB homologue, known as PkgB, or PKBR1 (Meili *et al*., 2000). This kinase protein is associated with the plasma membrane via myristoylation and not via a PH domain–PIP_3 interaction (Meili *et al*., 1999) and is activated by phosphorylation from TORC2 (Lee *et al*., 2005). We examined PKBR1 phosphorylation in *gskA* null mutant cells after cAMP stimulation, and found that as seen for PKBA, PKBR1 phosphorylation was also lost (Figure 4B). We could detect *PKBR1* expression (data not shown), suggesting a signaling failure upstream of PKBR1. In contrast to PKBA phosphorylation, PKBR1 phosphorylation was not restored by overexpression of IMPA (Figure 4B), indicating that this second molecular mechanism is independent of PIP_3 signaling. These results indicated that GskA is required for two intracellular signaling processes, explaining why it possesses a very strong chemotaxis defect.

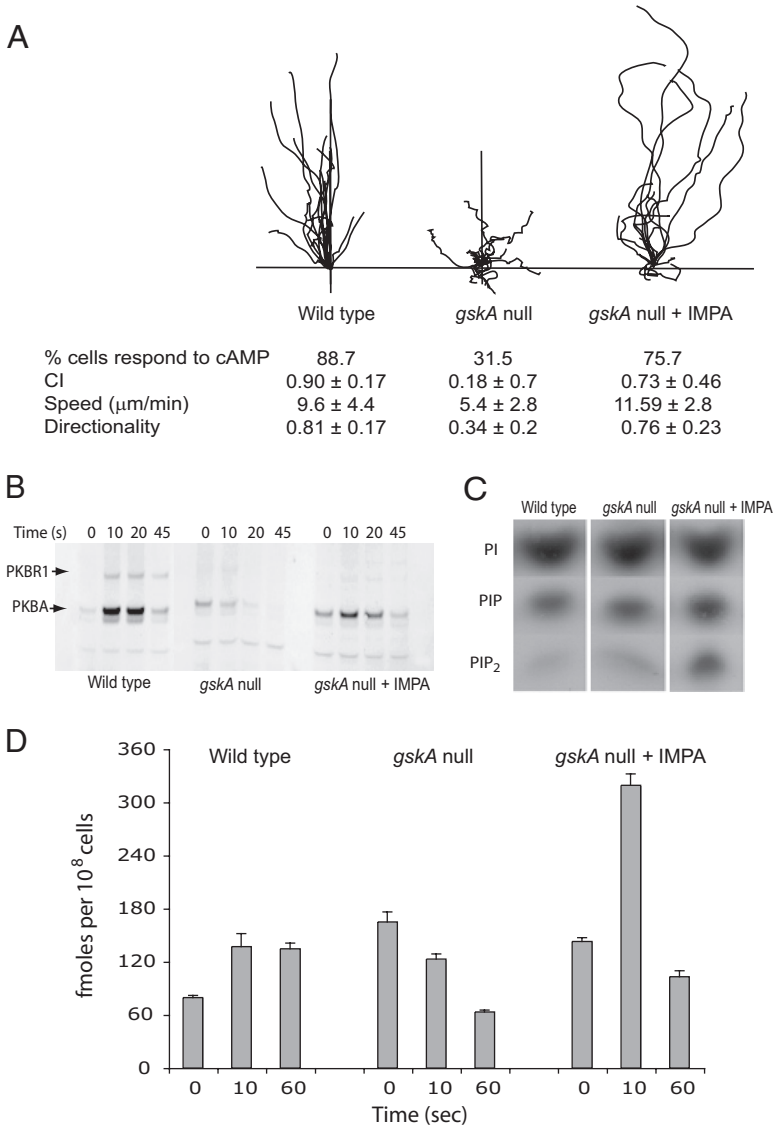

Figure 4. IMPA overexpression restores chemotaxis to *gskA* null mutant cells. (A) Comparison of wild-type cells and *gskA* null mutant cells overexpressing IMPA (*gskA* + IMPA) demonstrates rescued chemotaxis in the *gskA*-IMPA. (B) *gskA*-IMPA shows similar PKBA T278 phosphorylation kinetics to that observed in wild-type cells. However, T309 phosphorylation of PKBR1 is still absent after IMPA overexpression. (C) PI, PIP, and PIP_2 synthesis between fourth to fifth hour of early development show *gskA* mutant cells are still capable of producing phosphoinositides at levels similar to that of the wild type. (D) *gskA* mutant cells show higher basal PIP_3 levels compared with wild type; however, kinetics of PIP_3 synthesis do not reflect that shown in wild type and *gskA*-IMPA, post-cAMP stimulation.

gskA Null Mutants Have Impaired cAMP Synthesis

Although it restored chemotaxis, IMPA overexpression did not rescue aggregation or any other aspect of morphogenesis (Figure 5A and Supplemental Movie 2). This indicated that the aggregation defect was not a simple consequence of loss of chemotaxis, and may arise from an additional signaling deficiency. To test whether these cells can generate cAMP signals, cells were developed for 5 h in suspension and stimulated with the cAMP analogue 2-deoxyadenosine 3,5-monophosphate (dcAMP), and cAMP synthesis was measured. There was almost undetectable cAMP synthesis in *gskA* null- and *gskA* null-expressing IMPA cells (Figure 5B).

Dark-field optics was used to examine the cell signaling activity during aggregation. When viewed under these conditions, changes in cell shape in response to cAMP pulses can be seen as a change in light scattering (Tomchik and Devreotes, 1981). In wild-type cells, waves of light scattering propagate from the center of the aggregation field pass through the developing cell field as spiral waves (Figure 5C and Supplemental Movie 3A). In contrast to wild-type cells, no light scattering waves were observed in *gskA* null mutant cells or *gskA* mutants overexpressing IMPA (Figure 5C and Supplemental Movie 3B). These observations suggested that although PIP_3 signaling is sufficient to rescue chemotaxis, it was unable to restore cAMP signaling and fully rescue aggregation.

DISCUSSION

Here, we report that loss of GskA has substantial effects on *Dictyostelium* aggregation, causing a major defect in chemotaxis and cAMP signaling. This phenotype correlates with the presence of GskA activity during early stages of development and the results of previous microarray and proteomic analysis (Plyte *et al*., 1999; Strmecki *et al*., 2007). These results reveal an unexpectedly strong chemotaxis phenotype, which has been previously missed, and indicates that the terminal developmental phenotype of *Dictyostelium* mutants may not be a good indicator of defective chemotaxis.

Loss of *gskA* has a substantial effect on chemotaxis toward both cAMP and folate. These two chemotactic responses are mediated by different receptors and G proteins (Kumagai *et al*., 1989; Hadwiger *et al*., 1994; Kim *et al*., 1998). Together with the expression of the cAMP receptor *carA* and the

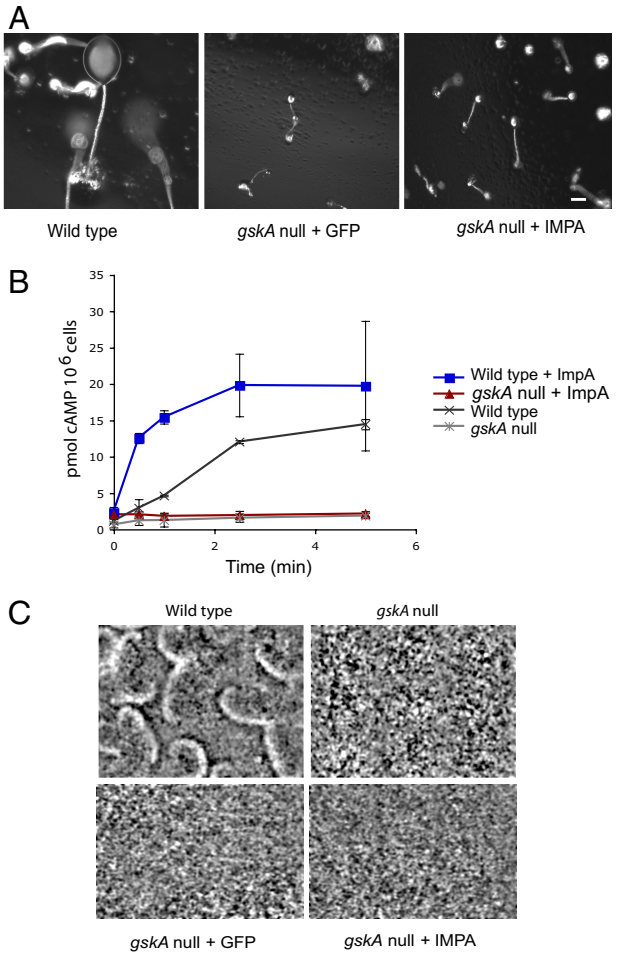

Figure 5. (A) Overexpression of IMPA in the *gskA* null background does not rescue aggregation and multicellular development. (B) cAMP production is impaired in both *gskA* null mutants and *gskA*-IMPA cell lines. (C) Dark-field images of aggregating wild-type cells at ≈3 h shows spirals of dark, stationary cells alternating with lighter areas of moving cells (top left). All *gskA* null mutant cell lines (null, *gskA*-GFP, and *gskA*-IMPA) do not show such patterning or light scattering waves. Bar, 50 μm.

presence of the PTEN response, these observations argue that the requirement for GskA lies at the level of effector activation rather than with signal sensing. We do not know exactly how loss of GskA inhibits folate chemotaxis, and our further conclusions are based on our investigation of the better characterized cAMP chemotaxis response.

We found that loss of *gskA* caused a major decrease in PIP_3 signaling, which could be bypassed by elevation of PIP_3 after overexpression of IMPA. Previous observations have shown that PIP_3 signaling is able to elicit the chemotaxis response (Kortholt *et al*., 2007), explaining how this restores chemotaxis to *gskA* null mutant cells. Although PIP_3 signaling is sufficient for chemotaxis, it is not essential and a simple loss of PIP_3 cannot totally explain the severe chemotaxis phenotype observed for the *gskA* null mutant cells. Loss or inhibition of PI3K or PIP_3 synthesis reduces speed and directionality in chemotaxing cells; however, it has only a minor effect on the CI value (Hoeller and Kay, 2007; King *et al*., 2009). In contrast, although we also saw reduced speed and directionality in the *gskA* null mutant, we also measured a large drop in the CI value. We found that loss of *gskA*

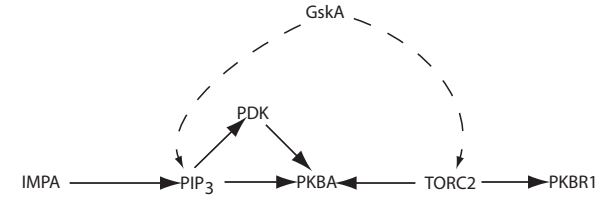

Figure 6. Proposed mechanism of GskA action on both PIP_3 and PKBR1. Phosphorylation of PKBA probably relies on both the action of TORC2 and another kinase, most likely PDK (Kamimura and Devreotes 2010, Liao *et al*., 2010), whereas GskA also acts upstream of TORC2, hence affecting subsequent phosphorylation of PKBR1.

blocks phosphorylation of PKBR1, a PIP_3-independent component of a parallel signaling pathway that also mediates chemotaxis to cAMP (Kolsch *et al*., 2008). We conclude that GskA acts upstream of both PIP_3- and PKBR1-mediated signaling (Figure 6).

In our experiments, we monitored PKBA and PKBR1 activation through antibodies specific to motifs phosphorylated by the protein kinase PDK-1 (Kamimura and Devreotes, 2010). This in turn is dependent on phosphorylation by TOR kinase as part of the TORC2 complex after cAMP stimulation. These events occur at the plasma membrane so that PKBR1 is dependent solely on TORC2 activation, whereas PKBA phosphorylation requires simultaneous TORC2 activation and PIP_3 synthesis. This presents a paradox: if TORC2 activation is required for both PKBA and PKBR1, how can overexpression of IMPA restore PKBA phosphorylation without an effect on PKBR1? We noted however that a small amount of PKBA phosphorylation occurs in the absence of TORC2. This is evident in the report from (Kamimura *et al*., 2008; Liao *et al*., 2010) where PKBA phosphorylation is observed in *pia* mutant cells, which lacks the *Dictyostelium* homologue of TORC2 component Rictor. We also observed PKBA phosphorylation in a *rip3* null mutant, lacking a second component of TORC2 (Supplemental Figure 1, top), but an absence of PKBR1 phosphorylation. We propose that elevation of PIP_3, as a consequence of IMPA overexpression, brings more PKBA to the membrane where it is phosphorylated through a TORC2-independent kinase. The identity of this kinase is not known, but a possible candidate could be the PDK1 homologue PdkA (Kamimura and Devreotes, 2010, Liao *et al*., 2010). Although both PdkA and its paralogue can function in the cytosol, PdkA can translocate to the plasma membrane in response to cAMP through binding to PIP_3 (Kamimura and Devreotes, 2010), and so IMPA overexpression could enhance PKBA phosphorylation by increasing the concentration of both PKBA and PdkA on the membrane. Furthermore, *PKBR1* null cells undergo normal chemotaxis (Meili *et al*., 2000), indicating that PKBA phosphorylation alone is sufficient for chemotaxis.

Further apparent complexity relates to earlier results concerning the effects of lithium on *Dictyostelium* chemotaxis. Lithium inhibits both GSK3 and IMPA (Van Lookeren Campagne *et al*., 1988; Van Dijken *et al*., 1996; Ryves *et al*., 1998; Ryves and Harwood, 2001) and therefore would be expected to produce the strong chemotaxis effect seen in the *gskA* null mutant. However, previously we found that lithium treatment of aggregation competent wild-type cells suppressed PIP_3 signaling, but left PKBR1 phosphorylation and cAMP synthesis unaffected (King *et al*., 2009). We demonstrated that this result arose from inhibition of IMPA, leading to a decrease in PIP_2 and subsequent PIP_3 synthesis. Arguing

against the possibility that GskA becomes insensitive to lithium, we found that nuclear export of Dd-STATa (Ginger *et al*., 2000), which is mediated by GskA phosphorylation, is suppressed by lithium in aggregation competent cells (Supplemental Figure 1, bottom left). We therefore propose that these differences arise through the timing of GskA action. Acute inhibition of GskA in aggregation competent cells, practically defined as cells pulsed with cAMP for 4 h before addition of lithium for 1 h, has no effect on chemotaxis or cAMP synthesis. In contrast, loss of GskA activity at the beginning of development or in growth phase cells causes the block to chemotaxis and signaling. In support of this hypothesis, we found that long-term treatment with lithium present from the initiation of cell development caused a substantial suppression of cAMP synthesis (Supplemental Figure 1, bottom right). This suggests that GskA activity acts as a permissive signal to initiate or set up chemotaxis but is not required continuously either as a direct requirement within the chemotaxis response or for maintenance of a chemotactic competent state. How GskA may achieve this is unclear; however, possibilities could range from constitutive phosphorylation of a protein that acts upstream of PIP_3 and TORC2 signaling to regulation of gene expression of a component, or components, required for chemotaxis and signaling.

What is clear is that GskA is required in the regulation of some aggregation-specific gene expression. Here, we have shown decreased expression in both *pdsA*, a cAMP phosphodiesterase, and *acaA*, the adenylyl cyclase required for generation of cAMP during aggregation. Loss of expression of these genes could account for loss of cAMP signaling during aggregation, but not the GskA requirement for chemotaxis. The earlier proteomic and microarray analysis of *gskA* null mutant cells (Strmecki *et al*., 2007) indicates several genes that may contribute to the chemotaxis phenotype. Loss of *gskA* reduces expression of *sodC*, a superoxide dismutase, which has been shown to be required for chemotaxis toward cAMP (Veeranki *et al*., 2008). The *sodC* mutant causes an increase in RasG activity even in the absence of cAMP stimulation, a known upstream activator of PI3-kinase (Sasaki *et al*., 2004), and could contribute to the higher basal levels of PKBA phosphorylation before cAMP stimulation (Figure 3). The microarray also showed that expression of the gene *alrA* is reduced in *gskA* null mutant cells. The AlrA, protein encodes an aldehyde reductase, which when disrupted also suppresses cell motility, although the mechanism is unclear (Ehrenman *et al*., 2004). Curiously, both GskA and AlrA have the capacity to alter glucose metabolism within the cell, but the significance of this is not known. In contrast, loss of *gskA* elevates expression of *ampA*. The product of this gene is antiadhesion protein that accumulates during aggregation (Varney *et al*., 2002), and elevated levels of AmpA could explain the instability of the small mounds observed during the aggregation of the *gskA* null.

Together, this study indicates that GskA is an important regulator of the aggregation process and is essential for cell chemotaxis. Our observations however also indicate that the role of GskA is probably complex, acting through a combination of mechanisms that are required at a minimum for chemotaxis and signaling but that also may include metabolism and cell adhesion. These may integrate to during early development to allow aggregation proceed to the multicellular stage, in which GskA mediates cell fate determination.

ACKNOWLEDGMENTS

We thank Peter D. Watson for invaluable help in creating the dark-field movies and advice related to microscopy. We also thank Gerry Weeks and Parvin Boulourani for advice regarding the folate experiments and Tsuyoshi Araki and Jeff Williams for the *Dictyostelium* monoclonal antibodies against STATa (D4). This work was funded by a Wellcome Trust Programme grant to A.J.H.

REFERENCES

Bloomfield, G., Tanaka, Y., Skelton, J., Ivens, A., and Kay, R. R. (2008). Widespread duplications in the genomes of laboratory stocks of *Dictyostelium discoideum*. Genome Biol. *9*, R75.

Cross, D. A., Alessi, D. R., Cohen, P., Andjelkovich, M., and Hemmings, B. A. (1995). Inhibition of glycogen synthase kinase-3 by insulin mediated by protein kinase B. Nature *378*, 785–789.

Curreli, N., Sollai, F., Massa, L., Comandini, O., Rufo, A., Sanjust, E., Rinaldi, A., and Rinaldi, A. C. (2001). Effects of plant-derived naphthoquinones on the growth of *Pleurotus sajor-caju* and degradation of the compounds by fungal cultures. J. Basic Microbiol. *41*, 253–259.

Ehrenman, K., Yang, G., Hong, W. P., Gao, T., Jang, W., Brock, D. A., Hatton, R. D., Shoemaker, J. D., and Gomer, R. H. (2004). Disruption of aldehyde reductase increases group size in *Dictyostelium*. J. Biol. Chem. *279*, 837–847.

Ginger, R. S., Dalton, E. C., Ryves, W. J., Fukuzawa, M., Williams, J. G., and Harwood, A. J. (2000). Glycogen synthase kinase-3 enhances nuclear export of a *Dictyostelium* STAT protein. EMBO J. *19*, 5483–5491.

Grimson, M. J., Coates, J. C., Reynolds, J. P., Shipman, M., Blanton, R. L., and Harwood, A. J. (2000). Adherens junctions and beta-catenin-mediated cell signalling in a non-metazoan organism. Nature *408*, 727–731.

Hadwiger, J. A., Lee, S., and Firtel, R. A. (1994). The G alpha subunit G alpha 4 couples to pterin receptors and identifies a signaling pathway that is essential for multicellular development in Dictyostelium. Proc. Natl. Acad. Sci. USA *91*, 10566–10570.

Harwood, A. J. (2001). Signal transduction and *Dictyostelium* development. Protist *152*, 17–29.

Harwood, A. J., Plyte, S. E., Woodgett, J., Strutt, H., and Kay, R. R. (1995). Glycogen synthase kinase 3 regulates cell fate in *Dictyostelium*. Cell *80*, 139–148.

Hellemans, J., Mortier, G., De Paepe, A., Speleman, F., and Vandesompele, J. (2007). qBase relative quantification framework and software for management and automated analysis of real-time quantitative PCR data. Genome Biol. *8*, R19.

Hoeller, O., and Kay, R. R. (2007). Chemotaxis in the absence of PIP3 gradients. Curr. Biol. *17*, 813–817.

Kamimura, Y., and Devreotes, P. N. (2010). Phosphoinositide-dependent protein kinase (PDK) activity regulates phosphatidylinositol 3,4,5-trisphosphate-dependent and -independent protein kinase B activation and chemotaxis. J. Biol. Chem. *285*, 7938–7946.

Kamimura, Y., Xiong, Y., Iglesias, P. A., Hoeller, O., Bolourani, P., and Devreotes, P. N. (2008). PIP3-independent activation of TorC2 and PKB at the cell's leading edge mediates chemotaxis. Curr. Biol. *18*, 1034–1043.

Kim, J. Y., Borleis, J. A., and Devreotes, P. N. (1998). Switching of chemoattractant receptors programs development and morphogenesis in *Dictyostelium*: receptor subtypes activate common responses at different agonist concentrations. Dev. Biol. *197*, 117–128.

Kim, L., Harwood, A., and Kimmel, A. R. (2002). Receptor-dependent and tyrosine phosphatase-mediated inhibition of GSK3 regulates cell fate choice. Dev. Cell *3*, 523–532.

Kim, L., Liu, J., and Kimmel, A. R. (1999). The novel tyrosine kinase ZAK1 activates GSK3 to direct cell fate specification. Cell *99*, 399–408.

King, J. S., Teo, R., Ryves, J., Reddy, J. V., Peters, O., Orabi, B., Hoeller, O., Williams, R. S., and Harwood, A. J. (2009). The mood stabiliser lithium suppresses PIP3 signalling in *Dictyostelium* and human cells. Dis. Model Mech. *2*, 306–312.

Kolsch, V., Charest, P. G., and Firtel, R. A. (2008). The regulation of cell motility and chemotaxis by phospholipid signaling. J. Cell Sci. *121*, 551–559.

Konig, S., Hoffmann, M., Mosblech, A., and Heilmann, I. (2008). Determination of content and fatty acid composition of unlabeled phosphoinositide species by thin-layer chromatography and gas chromatography. Anal. Biochem. *378*, 197–201.

Kortholt, A., King, J. S., Keizer-Gunnink, I., Harwood, A. J., and Van Haastert, P. J. (2007). Phospholipase C regulation of phosphatidylinositol 3,4,5-trisphosphate-mediated chemotaxis. Mol. Biol. Cell *18*, 4772–4779.

Kumagai, A., Pupillo, M., Gundersen, R., Miake-Lye, R., Devreotes, P. N., and Firtel, R. A. (1989). Regulation and function of G alpha protein subunits in *Dictyostelium*. Cell *57*, 265–275.

Lee, S., Comer, F. I., Sasaki, A., McLeod, I. X., Duong, Y., Okumura, K., Yates, J. R., 3rd, Parent, C. A., and Firtel, R. A. (2005). TOR complex 2 integrates cell movement during chemotaxis and signal relay in *Dictyostelium*. Mol. Biol. Cell *16*, 4572–4583.

Liao, X. H., Buggey, J., and Kimmel, A. R. (2010). Chemotactic activation of Dictyostelium AGC-family kinases AKT and PKBR1 requires separate but coordinated functions of PDK1 and TORC2. J. Cell Sci. *123*, 983–992.

Meili, R., Ellsworth, C., and Firtel, R. A. (2000). A novel Akt/PKB-related kinase is essential for morphogenesis in *Dictyostelium*. Curr. Biol. *10*, 708–717.

Meili, R., Ellsworth, C., Lee, S., Reddy, T. B., Ma, H., and Firtel, R. A. (1999). Chemoattractant-mediated transient activation and membrane localization of Akt/PKB is required for efficient chemotaxis to cAMP in *Dictyostelium*. EMBO J. *18*, 2092–2105.

Morio, T., *et al*. (1998). The Dictyostelium developmental cDNA project: generation and analysis of expressed sequence tags from the first-finger stage of development. DNA Res. *5*, 335–340.

Pan, P., Hall, E. M., and Bonner, J. T. (1972). Folic acid as second chemotactic substance in the cellular slime moulds. Nat. New Biol. *237*, 181–182.

Pan, P., Hall, E. M., and Bonner, J. T. (1975). Determination of the active portion of the folic acid molecule in cellular slime mold chemotaxis. J. Bacteriol. *122*, 185–191.

Papkoff, J., and Aikawa, M. (1998). WNT-1 and HGF regulate GSK3 beta activity and beta-catenin signaling in mammary epithelial cells. Biochem. Biophys. Res. Commun. *247*, 851–858.

Parent, C. A., Blacklock, B. J., Froehlich, W. M., Murphy, D. B., and Devreotes, P. N. (1998). G protein signaling events are activated at the leading edge of chemotactic cells. Cell *95*, 81–91.

Plyte, S. E., O'Donovan, E., Woodgett, J. R., and Harwood, A. J. (1999). Glycogen synthase kinase-3 (GSK-3) is regulated during *Dictyostelium* development via the serpentine receptor cAR3. Development *126*, 325–333.

Ryves, W. J., Fryer, L., Dale, T., and Harwood, A. J. (1998). An assay for glycogen synthase kinase 3 (GSK-3) for use in crude cell extracts. Anal. Biochem. *264*, 124–127.

Ryves, W. J., and Harwood, A. J. (2001). Lithium inhibits glycogen synthase kinase-3 by competition for magnesium. Biochem. Biophys. Res. Commun. *280*, 720–725.

Sasaki, A. T., Chun, C., Takeda, K., and Firtel, R. A. (2004). Localized Ras signaling at the leading edge regulates PI3K, cell polarity, and directional cell movement. J. Cell Biol. *167*, 505–518.

Schilde, C., Araki, T., Williams, H., Harwood, A., and Williams, J. G. (2004). GSK3 is a multifunctional regulator of *Dictyostelium* development. Development *131*, 4555–4565.

Snaar-Jagalska, B. E., and Van Haastert, P. J. (1994). G-protein assays in *Dictyostelium*. Methods Enzymol. *237*, 387–408.

Strmecki, L., Bloomfield, G., Araki, T., Dalton, E., Skelton, J., Schilde, C., Harwood, A., Williams, J. G., Ivens, A., and Pears, C. (2007). Proteomic and microarray analyses of the *Dictyostelium* Zak1-GSK-3 signaling pathway reveal a role in early development. Eukaryot. Cell *6*, 245–252.

Sun, T. J., and Devreotes, P. N. (1991). Gene targeting of the aggregation stage cAMP receptor cAR1 in *Dictyostelium*. Genes Dev. *5*, 572–582.

Takeda, K., Sasaki, A. T., Ha, H., Seung, H. A., and Firtel, R. A. (2007). Role of phosphatidylinositol 3-kinases in chemotaxis in *Dictyostelium*. J. Biol. Chem. *282*, 11874–11884.

Tomchik, K. J., and Devreotes, P. N. (1981). Adenosine 3′,5′-monophosphate waves in *Dictyostelium discoideum*: a demonstration by isotope dilution-fluorography. Science *212*, 443–446.

Van Dijken, P., Bergsma, J. C., Hiemstra, H. S., De Vries, B., Van Der Kaay, J., and Van Haastert, P. J. (1996). *Dictyostelium discoideum* contains three inositol monophosphatase activities with different substrate specificities and sensitivities to lithium. Biochem. J. *314*, 491–495.

Van Lookeren Campagne, M. M., Erneux, C., Van Eijk, R., and Van Haastert, P. J. (1988). Two dephosphorylation pathways of inositol 1,4,5-trisphosphate in homogenates of the cellular slime mould *Dictyostelium discoideum*. Biochem. J. *254*, 343–350.

Varney, T. R., Casademunt, E., Ho, H. N., Petty, C., Dolman, J., and Blumberg, D. D. (2002). A novel Dictyostelium gene encoding multiple repeats of adhesion inhibitor-like domains has effects on cell-cell and cell-substrate adhesion. Dev. Biol. *243*, 226–248.

Veeranki, S., Kim, B., and Kim, L. (2008). The GPI-anchored superoxide dismutase SodC is essential for regulating basal Ras activity and for chemotaxis of *Dictyostelium discoideum*. J. Cell Sci. *121*, 3099–3108.

Williams, J. G., Duffy, K. T., Lane, D. P., McRobbie, S. J., Harwood, A. J., Traynor, D., Kay, R. R., and Jermyn, K. A. (1989). Origins of the prestalk-prespore pattern in *Dictyostelium* development. Cell *59*, 1157–1163.

Williams, R. S., Eames, M., Ryves, W. J., Viggars, J., and Harwood, A. J. (1999). Loss of a prolyl oligopeptidase confers resistance to lithium by elevation of inositol (1,4,5) trisphosphate. EMBO J. *18*, 2734–2745.